

# “Regioselective Deposition” Method to Pattern Silver Electrodes Facilely and Efficiently with High Resolution: Towards All-Solution-Processed, High-Performance, Bottom-Contacted, Flexible, Polymer-Based Electronics

Deyang Ji, Lang Jiang,\* Yunlong Guo, Huanli Dong,\* Jianpu Wang, Huajie Chen, Qing Meng, Xiaolong Fu, Guofeng Tian, Dezhen Wu, Gui Yu,\* Yunqi Liu, and Wenping Hu\*

“Regioselectivity deposition” method is developed to pattern silver electrodes facilely and efficiently by solution-process with high resolution (down to 2  $\mu\text{m}$ ) on different substrates in A4 paper size. With the help of this method, large-area, flexible, high-performance polymer field-effect transistors based on the silver electrodes and polyimide insulator are fabricated with bottom-contact configuration by all-solution processes. The polymer devices exhibit high performance with average field-effect mobility over  $1.0\text{ cm}^2\text{ V}^{-1}\text{ s}^{-1}$  (the highest mobility up to  $1.5\text{ cm}^2\text{ V}^{-1}\text{ s}^{-1}$ ) and excellent environmental stability and flexibility, indicating the cost effectiveness of this method for practical applications in organic electronics.

potential as a cheap alternative to amorphous silicon-based thin-film transistors.<sup>[1]</sup> Development of low-cost, flexible and large-area OFETs is a prerequisite for integrating them into future commercial applications, such as e-paper, radio frequency identification (RFID) tags, smart cards, and addressing back-planes in displays.<sup>[2]</sup> Solution-processed manufacturing techniques (involving the fabrication of gate and source/drain electrodes, insulator, and organic semiconductor) are effective approaches to achieve large-area, low-cost and flexible electronic devices. Although there

## 1. Introduction

Organic field-effect transistors (OFETs) have stimulated great interest in the past decade due to their technological

have been substantial researches based on a combination of solution processing and evaporation methods,<sup>[3,4]</sup> which still restricts the development and application of organic electronic to a great extent. To date, all-solution-processed OFETs have been rarely addressed,<sup>[5,1b]</sup> and their device performances are still unsatisfactory ( $<0.5\text{ cm}^2\text{ V}^{-1}\text{ s}^{-1}$ ). Possible reasons for this issue include factors of electrode materials, patterning technique, resolution and solvent effect. Although various materials<sup>[1b,5d,6]</sup> have been processed in solution to serve as electrodes, their low conductivity, high annealing temperature ( $>120\text{ }^\circ\text{C}$ ) and high prices of the raw materials limit their further applications. Moreover, OFETs based on bottom-gate bottom-contact configuration, the preparation of source/drain electrodes and organic active layers by solution-process can easily damage organic gate dielectric layers. In addition, although individual miniaturized OFETs have been fabricated by regulating and controlling the surface energy of the droplets,<sup>[7]</sup> large-area, high-resolution, all-solution-processed OFET arrays are still a great challenge.

Silver mirror reaction is a straightforward way to produce silver films, and it has been widely used in glass industry. The reaction can be realized by cheap reactants in beakers with the aqueous solution at room temperature, and the silver film can be deposited on any materials without substrate dependence. These advantages make it attractive to fabricate metal electrodes. But the reaction is hard to control, and it tends to

D. Ji, Dr. L. Jiang, Dr. Y. Guo, Dr. H. Dong, Dr. H. Chen, Dr. Q. Meng, X. Fu, Prof. G. Yu, Prof. Y. Liu, Prof. W. Hu  
Beijing National Laboratory for Molecular Sciences  
Key Laboratory of Organic Solids  
Institute of Chemistry  
Chinese Academy of Sciences  
Beijing 100190, China  
E-mail: dhl522@iccas.ac.cn; yugui@iccas.ac.cn; huwp@iccas.ac.cn



D. Ji, X. Fu  
University of Chinese Academy of Sciences  
Beijing 100039, China  
Dr. L. Jiang, Dr. J. Wang  
Cavendish Laboratory  
Cambridge University  
JJ Thomson Avenue  
Cambridge, CB3 0HE, UK  
E-mail: lj307@cam.ac.uk  
Dr. H. Dong, Prof. W. Hu  
Collaborative Innovation Center of Chemical Science and Engineering  
Tianjin 300072, China  
Dr. G. Tian, Prof. D. Wu  
Beijing University of Chemical Technology  
Beijing 100029, China

DOI: 10.1002/adfm.201304117

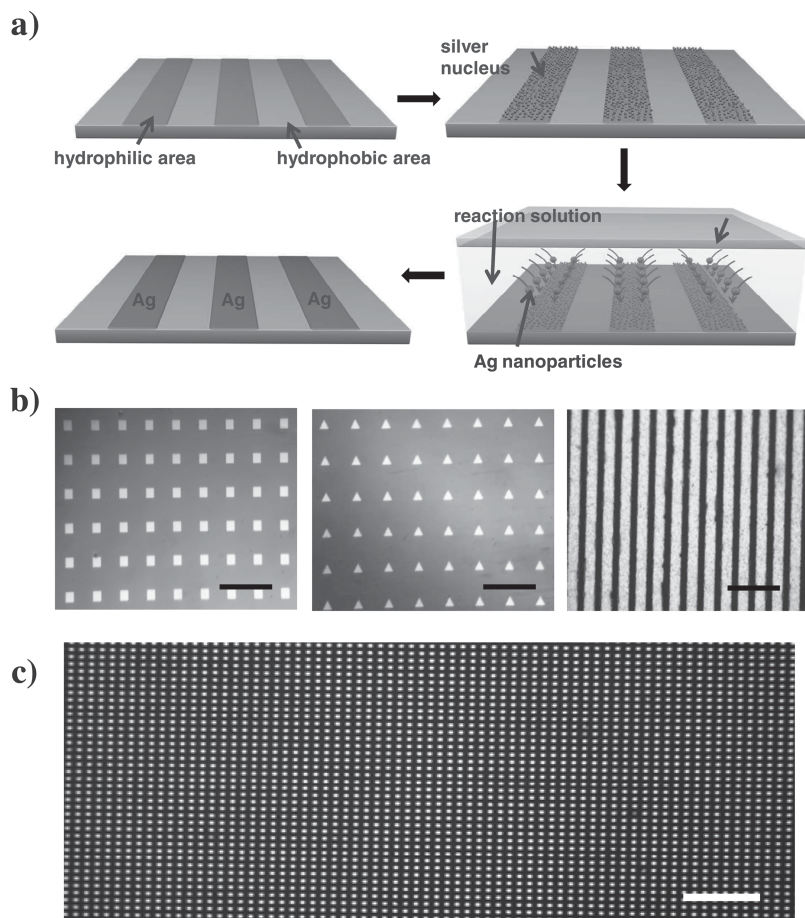


**Figure 1.** a) The schematic process of regioselective deposition for silver electrodes, b) different silver arrays (square, triangle and strip-type arrays) patterned on glass, the scale bar is 100  $\mu\text{m}$ , 100  $\mu\text{m}$ , 20  $\mu\text{m}$ , respectively, c) high-resolution silver dot arrays patterned on glass, the diameter of the silver dot is 5  $\mu\text{m}$ , the scale bar is 75  $\mu\text{m}$ .

quickly deposit everywhere, which makes it difficult for OFET applications. An improved silver mirror reaction is necessary to produce silver electrodes or inks (for ink-jet printing)<sup>[8]</sup> to avoid the high annealing temperature (120–200  $^{\circ}\text{C}$ ) (to obtain good conductivity of the silver films) and low device mobility ( $<0.1 \text{ cm}^2 \text{ V}^{-1} \text{ s}^{-1}$ ). Here, we demonstrate a new approach, “regioselective deposition”, to pattern silver electrodes facily and efficiently with high resolution.

## 2. Results and Discussion

### 2.1. Controlled Silver Mirror Reaction at the Room Temperature

To our best knowledge, silver mirror reaction is too rapid to keep it at solution state with the reaction temperature about 100  $^{\circ}\text{C}$ , and may form nanoparticles before dropping on the substrate. Moreover, the thickness and the roughness of the silver film are also hard to control. Therefore, how to control the reaction rate to grow thin and low roughness silver film still remains a challenge. Here we slowed down the reaction rate by decreasing reaction temperature at room temperature. By

further changing reaction time and tuning the reaction volumes, the thickness and the roughness of the silver film can be well controlled. In our work, because all the process of silver mirror reaction is mild, the reaction solution can be controlled at solution state more easily before dropping it on the substrate at room temperature. What's more, the rate of silver nanoparticles depositing on the substrate is also slow leading to close accumulation of silver nanoparticles formed on the substrate. In addition, the smooth surface of the substrate (Figure S1, Supporting Information) is more conducive to lower surface roughness. The thickness from 60 nm to 200 nm is shown in Figure S2 (Supporting Information) and the roughness depends on the thickness shown in Figure S3 (Supporting Information). The roughness of the silver film can be well-controlled around 20 nm ( $R_q$ ), or even lower roughness around 10 nm (Figure S4, Supporting Information), which is significantly lower than the roughness of previously reported solution-processed silver films.<sup>[8]</sup>

### 2.2. “Regioselective Deposition” Method

A new and facile process called “regioselective deposition” method is developed to prepare the pattern of silver films. The “regioselective deposition” method can be divided into several steps as shown in Figure 1a. The focus of the technique is by controlling the reaction on substrate designed area through hydrophobic/hydrophilic reaction.

For example, the surfaces of OTS-modified  $\text{SiO}_2/\text{Si}$  and polyimide substrates are hydrophobic with contact angles of 105 $^{\circ}$  and 94 $^{\circ}$  respectively (Figure S5a,b, Supporting Information), which can be shifted to hydrophilic with contact angles of 8 $^{\circ}$  and 19 $^{\circ}$  after oxygen plasma treatment (Figure S5c,d, Supporting Information). Therefore, by plasma treatment with a shadow mask, the substrates can be divided into hydrophilic and hydrophobic patterns easily. Silver nuclei can be generated on the hydrophilic area by dipping the target substrate into the reaction solution. Then, another hydrophilic substrate after dipped in the reaction solution for a while is put on the top of the target substrate serving as silver source to aid further growth of the silver nuclei into films (60–80 nm). Depending on the aqueous solution reaction and the limit of silver source, silver can only selectively grow in the hydrophilic area.<sup>[9]</sup> Figure 1b shows various silver patterns (square and triangle) arrays with 20  $\mu\text{m}$  length of side prepared by using this regioselective deposition method on the glass substrate, and silver electrode arrays (strip-type) with high resolution (2  $\mu\text{m}$ ). High-resolution silver dot arrays were also patterned facily and efficiently on the glass substrate with the diameter of 5  $\mu\text{m}$  (Figure 1c).

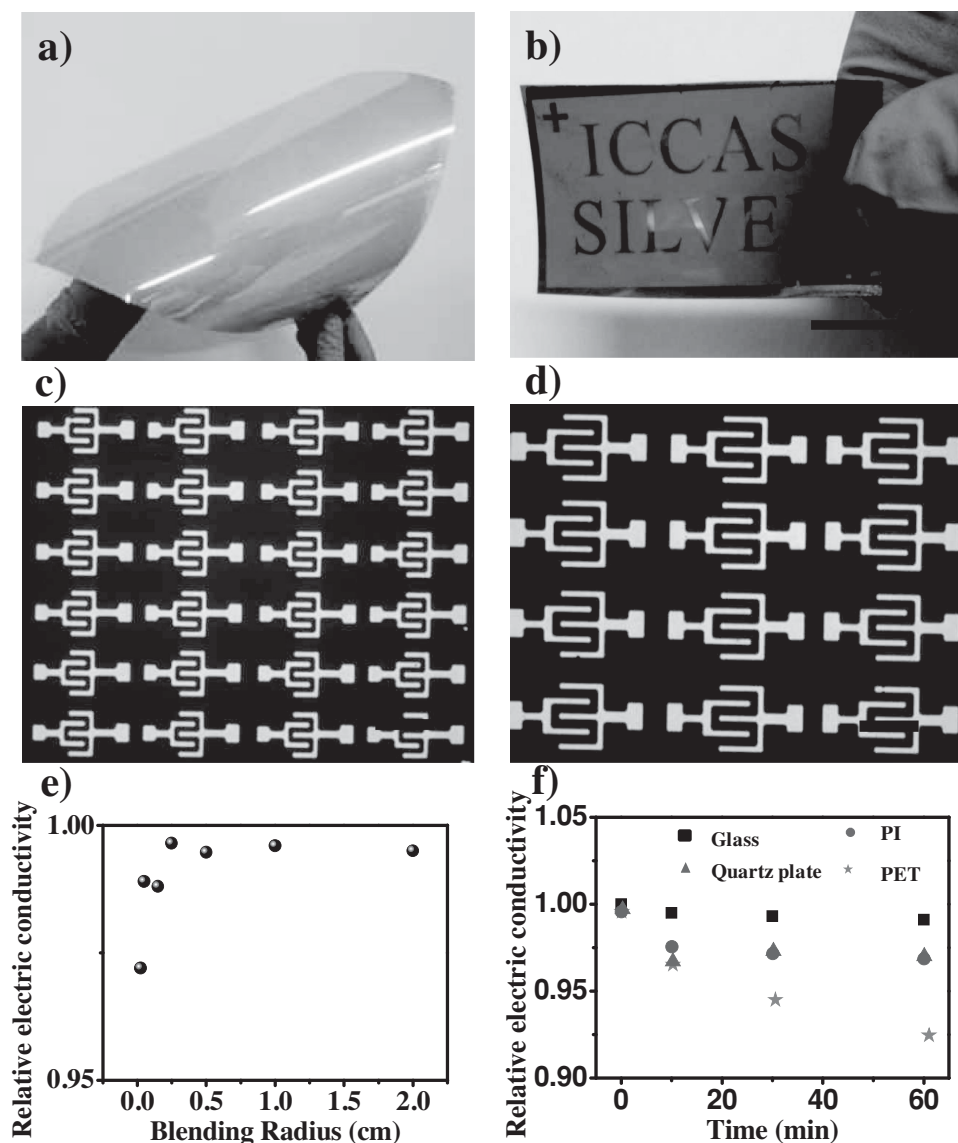


**Figure 2.** a) Large-area silver film (25 cm × 20 cm, ≈A4 size) on flexible polyimide, b) alphabet “ICCAS SILVER” pattern (4 cm × 2 cm), the scale bar is 1 cm, c) silver electrodes with channel length of 5 μm on the polyimide substrate, the scale bar is 50 μm, d) silver electrodes with channel length of 10 μm on the polyimide substrate, the scale bar is 80 μm, e) plots of conductivity versus bending conditions on polyimide (PI) substrate, f) plots of conductivity of the silver electrodes on different substrates versus ultrasound time in ethanol.

### 2.3. Manufacture of Solution Processed Silver Electrode

The patterning of silver electrodes on flexible substrate is shown in **Figure 2**. Polyimide is chosen as the substrate because of its high dielectrics and excellent insolubility in common organic solvents. In our experiment, the 1 μm polyimide dielectric layer (with the capacitance of 3.6 nF cm<sup>-2</sup>) is formed by crosslinking the spin-coated film of polyimide precursor<sup>[10]</sup> at 300 °C. Figure 2a shows the obtained silver film on polyimide substrate in large area and it demonstrates nice flexibility (large area and folded silver films shown in Figure S6). By using “regioselective deposition” method silver could be accurately defined in the desired position. As shown in Figure 2b, nice alphabet of “ICCAS SILVER” is patterned

facilely on the flexible polyimide substrate (4 cm × 2 cm), and silver electrode arrays for OFETs are patterned efficiently on polyimide as shown in Figure 2c (5 μm channel length) and Figure 2d (10 μm channel length). It should be noted that the silver electrodes exhibit excellent electrical conductivity ( $(1 \pm 0.2) \times 10^5$  S cm<sup>-1</sup>) at room temperature, which is comparable with that of bulk silver ( $6.25 \times 10^5$  S cm<sup>-1</sup>). As shown in Figure 2e, with the bending of the substrate, although the conductivity has slightly decline, it remains high conductivity with a bending radius as small as 0.25 mm, demonstrating the excellent flexibility and robust mechanical properties of the electrodes. More important, the electrodes adhere on the different substrates extremely tightly. Here four substrates (glass, quartz glass, polyimide (PI) and polyethylene



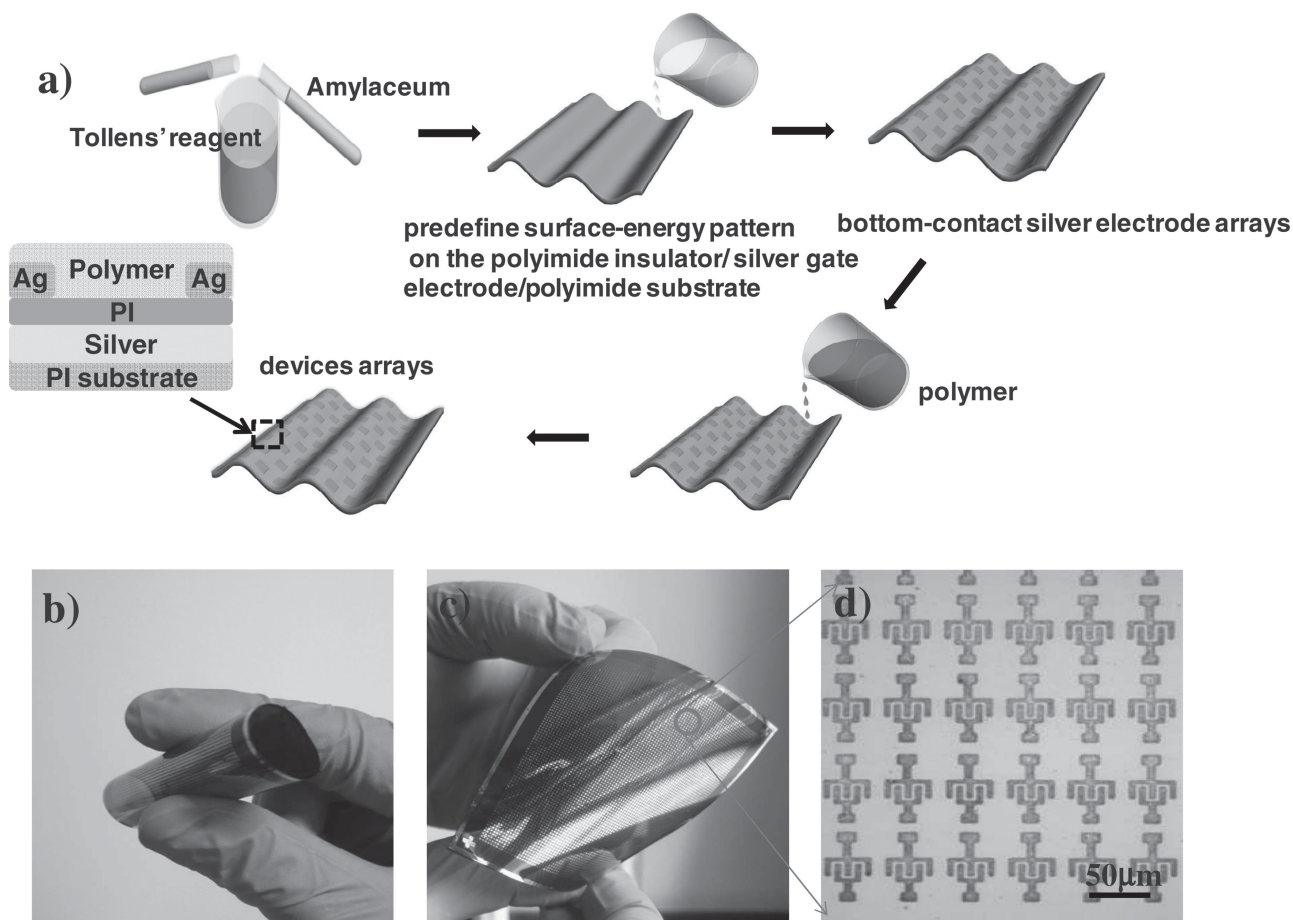


**Figure 3.** a) The flow chart of preparing large-area all-solution-processed flexible OFET arrays, b) the curled-up flexible OFET arrays, c) the layout of flexible OFET arrays, d) an enlarged image of the device arrays in Figure 3c.

terephthalate (PET)) (Figure 2f) are adopted to be deposited with the silver film using silver mirror reaction at room temperature after their surface hydrophilic treatment (plasma, 40 W, 5 min). The conductivity decreases less than 5% for glass, quartz glass and polyimide (PI) and 8% for PET, even after ultrasonication (40 W) in ethanol for one hour. These advantages indicate their great potential for flexible electronics.

## 2.4. Fabrication of Flexible All-Solution-Processed OFETs and Their Characterization

The fabrication of large-area, all-solution-processed, high-performance OFETs and OFET arrays based on the “regioselective deposition” and flexible substrate is shown in **Figure 3a** and its corresponding cross-sectional illustration of the ultimate device is shown in the inset of Figure 3a. Spin-coated polymer PDVT-10 was selected as the organic semiconducting layer due to its high mobility and air-stability.<sup>[3d]</sup> Figure 3b shows the fabricated curled up OFET arrays, and Figure 3c shows the layout of the flexible OFET arrays, and an enlarged drawing

of the device arrays is shown in Figure 3d. It should be noted that Ag electrodes have a work function of 4.7 eV, which does not match the HOMO energy level of PDVT-10 ( $\approx 5.28$  eV),<sup>[3d]</sup> leading to large injection barrier. Therefore, solution-processed 7, 7', 8, 8'-tetracyanoquinodimethane (TCNQ) could be used to modify the work function of the silver by forming AgTCNQ.<sup>[11]</sup>

**Figure 4a** shows the structure of the fabricated flexible all-solution-processed OFET with a typical bottom-gate, bottom-contact device configuration. The OFET devices (channel length: 5  $\mu\text{m}$ , channel width: 30  $\mu\text{m}$ ) on flexible polyimide substrates exhibit high performance with uniform mobility. Representative transfer and output characteristics of the transistors based on PDVT-10 are shown in Figure 4b,c. Devices in any part of the substrate show similar performance, and the mobility distribution is presented in Figure 4d. The average mobility in the saturated regime is  $1.0 \text{ cm}^2 \text{ V}^{-1} \text{ s}^{-1}$  and the highest mobility reaches as high as  $1.5 \text{ cm}^2 \text{ V}^{-1} \text{ s}^{-1}$  with ON/OFF  $(3 \pm 2) \times 10^4$  and threshold voltage  $(6 \pm 2) \text{ V}$ . The mobility value is significantly higher than earlier reported results of all-solution-processed flexible OFETs.<sup>[5,1b]</sup> Moreover, the devices show good air stability. As shown in Figure 4e, no obvious degradation of the device performance is observed in all devices

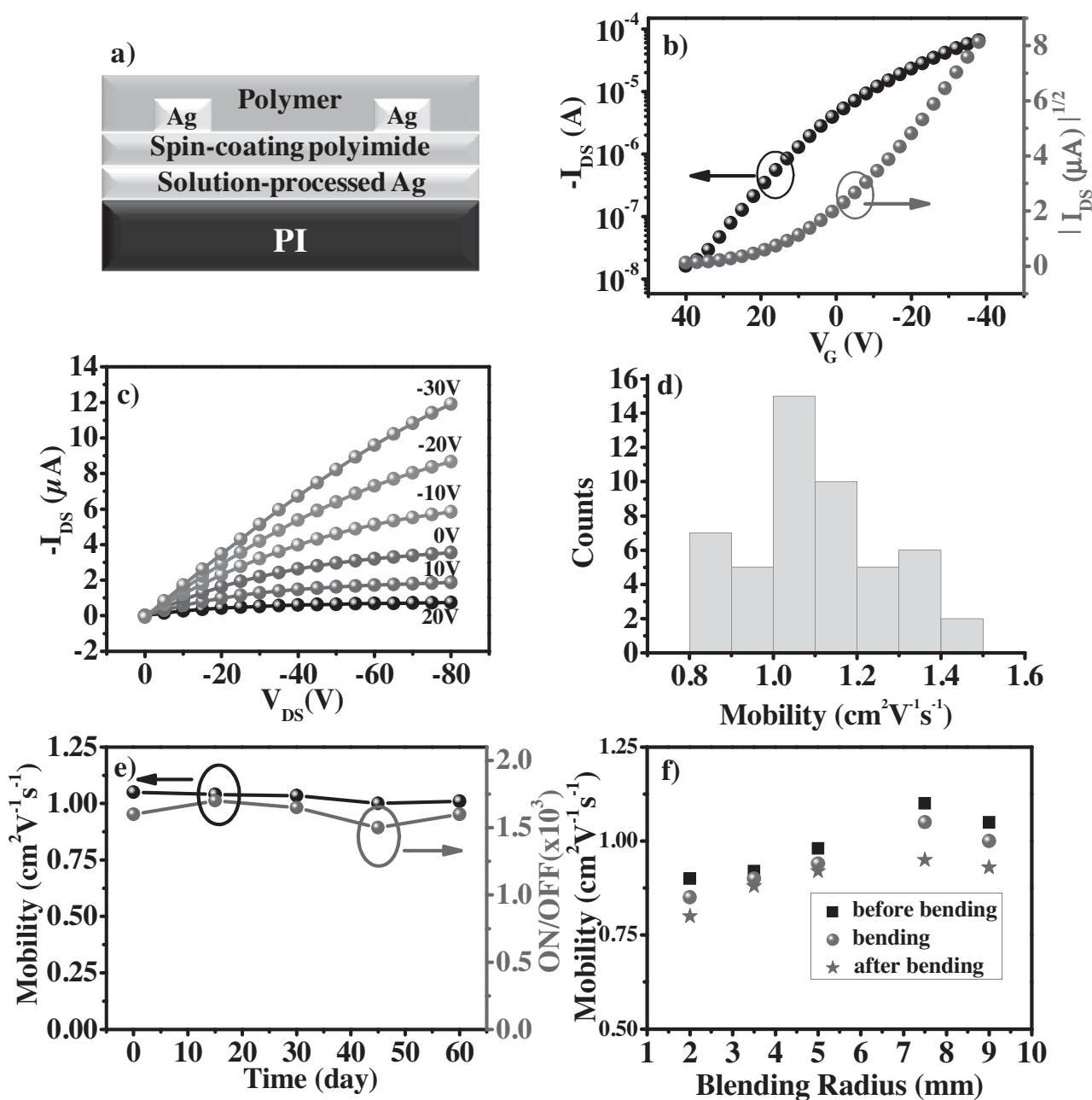


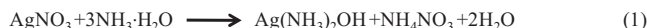
**Figure 4.** a) Device structure of all-solution-processed OFETs, b) typical transfer characteristics of the transistor based on PVDT-10 on polyimide substrate, c) typical output characteristics of the transistor based on PVDT-10 on polyimide substrate, d) distribution of the mobility for devices by all-solution process, e) the shelf-life test based on the devices, f) plots of mobility versus bending radius on polyimide (PI) substrate.

over 60 days with outside humidity at least 50%. To test the device flexibility, OFET arrays on the polyimide substrates were bent to various radii (0.2 cm, 0.35 cm, 0.5 cm, 0.75 cm, and 0.9 cm) by using different cylindrical objects. Here, the devices were on the outside wall of the bent cylinder. Figure 4f shows a plot of the mobility versus bending radius. Little difference about the average mobilities of the OFET array is observed before, during, and after bending. However, with the bending radii decreasing, the average mobilities have a tendency to

reduce less than 20%. All the results indicate the huge potential of this novel technique in the application of organic flexible electronics.

### 3. Conclusion

We have developed a facile “regioselective deposition” technique to pattern silver electrodes with high resolution and low



**Scheme 1.** The equation of the synthetic process of silver films.

cost. Flexible, large-area and high-performance polymer transistors have been fabricated through all-solution processes based on this technique. The mobility of the flexible and all-solution-processed polymer transistors was as high as  $1.5 \text{ cm}^2 \text{ V}^{-1} \text{ s}^{-1}$ . Together with the high flexibility, excellent uniformity and low cost, this technique demonstrates promising applications in the organic electronics industry.

## 4. Experimental Section

**The Process of Silver Mirror Reaction:** the silver mirror reaction (shown in **Scheme 1**) is performed in aqueous ammonia, silver nitrate and amylaceum to directly fabricate the silver thin films. Specifically, an aqueous ammonia solution was first added into 5 mL silver nitrate aqueous solution (2%) drop by drop. Then, 5 mL amylaceum aqueous solution (10 mg mL) was thoroughly mixed with the reaction mixture in a beaker and subsequently dropped onto the surface of the substrates at room temperature ( $25^\circ\text{C}$ ) to form the silver film. The reaction can be easily scaled up to prepare silver films in larger vessels, for example, 500 mL beaker (Figure S7, Supporting Information).

**Substrates Cleaning:** Glass substrates used in the present study were successively cleaned with pure water, acetone, pure ethanol, piranha solution ( $\text{H}_2\text{SO}_4 : \text{H}_2\text{O}_2 = 7 : 3$ ), pure water, hot ammonia-hydrogen peroxide solution (ammonia: hydrogen peroxide: water = 1 : 1 : 5), pure water and pure ethanol. Polyimide flexible substrates used in the present study were successively cleaned with pure water, acetone, and pure ethanol.

**Hydrophilic/Hydrophobic Pattern and Plasma Treatment:** the resolution of the pattern above 30 micrometers can be achieved by oxygen plasma under a shadow mask. The shadow mask was first placed on the hydrophobic surface, and oxygen plasma treatment (40 W, 30 s) was then performed to create the hydrophilic/hydrophobic pattern. The resolution of the pattern below 30 micrometers can be achieved by a high-resolution patterning method, such as photolithography and soft lithography. In the present study, we used photolithography technology. A photoresist layer was spin-coated onto the polyimide insulating (hydrophobic) layer, which subsequently was exposed and developed to form a high-resolution pattern. Following that, the surface was treated with oxygen plasma (40 W, 30 s). Finally, the photoresist was rinsed off with acetone to obtain the hydrophilic/hydrophobic pattern. The resolution of the electrode channel length was limited by the resolution of the photoresist. In this work, the highest resolution of the electrode channel length was  $2 \mu\text{m}$ . Positive photo resist (RZJ-304) and the developer were purchased from Ruihong in China. The main composition of the developer is tetramethyl ammonium hydroxide (TMAH, 2.38%), while the solvent is water.

**Measurements:** The electrical characteristics of the OFET devices were recorded at room temperature in air by using a Keithley 4200 SCS semiconductor parameter analyzer and a Micromanipulator 6150 probe station. Atomic force microscopy (AFM) was performed using a Nanoscopy IIIa instrument (USA). Plasma treatment was carried out using Gala Instrument Prep2.

## Supporting Information

Supporting Information is available from the Wiley Online Library or from the author.

## Acknowledgments

The authors acknowledge financial support from National Natural Science Foundation of China (51033006, 51222306, 51003107, 91233205, 91222203, 91027043, 61201105), the China-Denmark Co-project, TRR61 (NSFC-DFG Transregio Project), the Ministry of Science and Technology of China (2011CB808400, 2013CB933403, 2011CB932300, 2013 CB933500) and the Chinese Academy of Sciences. The authors are grateful to Tao Li (Copenhagen University) and Christopher Warwick (University of Cambridge) for profound discussions.

Received: December 9, 2013

Revised: January 12, 2014

Published online: February 20, 2014

- [1] a) Z. Bao, Y. Feng, A. Dodabalapur, V. R. Raju, A. J. Lovinger, *Chem. Mater.* **1997**, *9*, 1299; b) H. Sirringhaus, T. Kawase, R. H. Friend, T. Shimoda, M. Inbasekaran, W. Wu, E. P. Woo, *Science* **2000**, *290*, 2123; c) M. Halik, H. Klauk, U. Zschieschang, G. Schmid, W. Radlik, W. Weber, *Adv. Mater.* **2002**, *14*, 1717; d) K. Takimiya, H. Ebata, K. Sakamoto, T. Izawa, T. Otsubo, Y. Kunugi, *J. Am. Chem. Soc.* **2006**, *128*, 12604; e) K. C. Dickey, J. E. Anthony, Y. L. Loo, *Adv. Mater.* **2006**, *18*, 1721; f) T. Izawa, E. Miyazaki, K. Takimiya, *Adv. Mater.* **2008**, *20*, 3388; g) H. Yan, Z. Chen, Y. Zheng, C. Newman, J. R. Quinn, F. Dötz, M. Kastler, A. Facchetti, *Nature* **2009**, *457*, 679; h) M. E. Roberts, N. Queraltó, S. C. B. Mannsfeld, B. N. Reinecke, W. Knoll, Z. Bao, *Chem. Mater.* **2009**, *21*, 2292; i) Y. Ito, A. A. Virkar, S. Mannsfeld, J. H. Oh, M. Toney, J. Locklin, Z. Bao, *J. Am. Chem. Soc.* **2009**, *131*, 9396; j) K. Liao, A. G. Ismail, L. Kreplak, J. Schwartz, I. G. Hill, *Adv. Mater.* **2010**, *22*, 3081; k) D. Ji, L. Jiang, H. Dong, Q. Meng, Z. Wang, H. Zhang, W. Hu, *ACS Appl. Mater. Interf.* **2013**, *5*, 2316.
- [2] a) M.-H. Yoon, H. Yan, A. Facchetti, T. J. Marks, *J. Am. Chem. Soc.* **2005**, *127*, 10388; b) H. Klauk, *Organic Electronics: Materials, Manufacturing, and Applications* Wiley-VCH, Weinheim, Germany **2006**; c) Z. Bao, J. John Locklin, *Organic field-effect transistors* CRC press, Boca Raton, FL **2007**; d) S. C. B. Mannsfeld, B. C. K. Tee, R. M. Stoltenberg, C. V. H. H. Chen, S. Barman Beinn, V. O. Muir, A. N. Sokolov, C. Reese, Z. N. Bao, *Nat. Mater.* **2010**, *9*, 859; e) Y. Wen, Y. Liu, Y. Guo, G. Yu, W. Hu, *Chem. Rev.* **2011**, *111*, 3358; f) C. Wang, H. Dong, W. Hu, Y. Liu, D. Zhu, *Chem. Rev.* **2012**, *112*, 2208.
- [3] a) T. Izawa, E. Miyazaki, K. Takimiya, *Adv. Mater.* **2008**, *20*, 3388; b) M. J. Kang, I. Doi, H. Mori, E. Miyazaki, K. Takimiya, M. Ikeda, H. Kuwabara, *Adv. Mater.* **2011**, *23*, 1222; c) G. Giri, E. Verploegen, S. C. B. Mannsfeld, S. A. Evrenk, D. H. Kim, S. Y. Lee, H. A. Becerril, A. A. Guzik, M. F. Toney, Z. Bao, *Nature* **2011**, *480*, 504; d) H. Chen, Y. Guo, G. Yu, Y. Zhao, J. Zhang, D. Gao, H. Liu, Y. Liu, *Adv. Mater.* **2012**, *24*, 4618; e) L. Huang, M. Stolte, H. Bückstümmer, F. Würthner, *Adv. Mater.* **2012**, *24*, 5750; f) J. Li, Y. Zhao, H. S. Tan, Y. Guo, C. Di, G. Yu, Y. Liu, M. Lin, S. H. Lim, Y. Zhou, H. Su, B. S. Ong, *Sci. Rep.* **2012**, *2*, 754.
- [4] a) T. Lee, Y. Byun, B. Koo, I. Kang, Y. Lyu, C. H. Lee, L. Pu, S. Y. Lee, *Adv. Mater.* **2005**, *17*, 2180; b) P. Liu, Y. Wu, Y. Li, B. S. Ong, S. Zhu, *J. Am. Chem. Soc.* **2006**, *128*, 4554.
- [5] a) C. J. Drury, C. M. J. Mutsaers, C. M. Hart, M. Matters, D. M. Leeuw, *Appl. Phys. Lett.* **1998**, *73*, 108; b) G. H. Gelinck, T. C. T. Geuns, D. M. Leeuw, *Appl. Phys. Lett.* **2000**, *77*, 1487; W. H. Lee, J. A. Lim, D. Kwak, J. H. Cho, H. S. Lee, H. H. Choi, K. Cho, *Adv. Mater.* **2009**, *21*, 4243; c) M. Kano, T. Minari, K. Tsukagoshi, *Appl. Phys. Express* **2010**, *3*, 051601; d) Y. Zhao, C. Di, X. Gao, Y. Hu, Y. Guo, L. Zhang, Y. Liu, J. Wang, W. Hu, D. Zhu, *Adv. Mater.* **2011**, *23*, 2448.

- [6] a) S. Lim, B. Kang, D. Kwak, W. H. Lee, J. A. Lim, K. Cho, *J. Phys. Chem. C* **2012**, 116, 7520; b) L. Zhang, H. Liu, Y. Zhao, X. Sun, Y. Wen, Y. Guo, X. Gao, C. Di, G. Yu, Y. Liu, *Adv. Mater.* **2012**, 24, 436.
- [7] a) H. Sirringhaus, T. Kawase, R. H. Friend, T. Shimoda, M. Inbasekaran, W. Wu, E. P. Woo, *Science* **2000**, 290, 2123; b) J. Z. Wang, Z. H. Zheng, H. W. Li, W. T. S. Huck, H. Sirringhaus, *Nat. Mater.* **2004**, 3, 171; c) C. W. Sele, T. V. Werne, R. H. Friend, H. Sirringhaus, *Adv. Mater.* **2005**, 17, 997; d) N. Zhao, M. Chiesa, H. Sirringhaus, Y. Li, Y. Wu, B. Ong, *J. Appl. Phys.* **2007**, 101, 064513; e) Y. Noh, N. Zhao, M. Caironi, H. Sirringhaus, *Nature Nanotechnol.* **2007**, 2, 784; f) M. Caironi, E. Gili, T. Sakanoue, X. Cheng, H. Sirringhaus, *ACS Nano* **2010**, 4, 1451.
- [8] a) Y. Li, Y. Wu, B. S. Ong, *J. Am. Chem. Soc.* **2005**, 127, 3266; b) Y. Wu, Y. Li, B. S. Ong, *J. Am. Chem. Soc.* **2006**, 128, 4202; c) Y. Wu, Y. Li, B. S. Ong, *J. Am. Chem. Soc.* **2007**, 129, 1862; d) S. B. Walker, J. A. Lewis, *J. Am. Chem. Soc.* **2008**, 130, 1419.
- [9] S. Huang, A. W. H. Mau, *J. Phys. Chem. B* **2003**, 107, 3455.
- [10] a) J. Zhan, Z. Wu, S. Qi, D. Wu, W. Yang, *Thin Solid Films* **2011**, 519, 1960; b) D. Ji, L. Jiang, X. Cai, H. Dong, Q. Meng, G. Tian, D. Wu, J. Li, W. Hu, *Org. Electron.* **2013**, 14, 2528.
- [11] a) C. Di, G. Yu, Y. Liu, X. Xu, D. Wei, Y. Song, Y. Sun, Y. Wang, D. Zhu, J. Liu, D. Wu, *J. Am. Chem. Soc.* **2006**, 128, 16418; b) J.-P. Hong, A.-Y. Park, S. Lee, J. Kang, N. Shin, D. Y. Yoon, *Appl. Phys. Lett.* **2008**, 92, 143311; c) K.-Y. Wu, S.-Y. Yu, Y.-T. Tao, *Langmuir* **2009**, 25, 6232; d) G. L. Whiting, A. C. Arias, *Appl. Phys. Lett.* **2009**, 95, 253302; e) H. Chen, I. Wu, C. Chen, S. Liu, C. Wu, *Org. Electron.* **2012**, 13, 593.